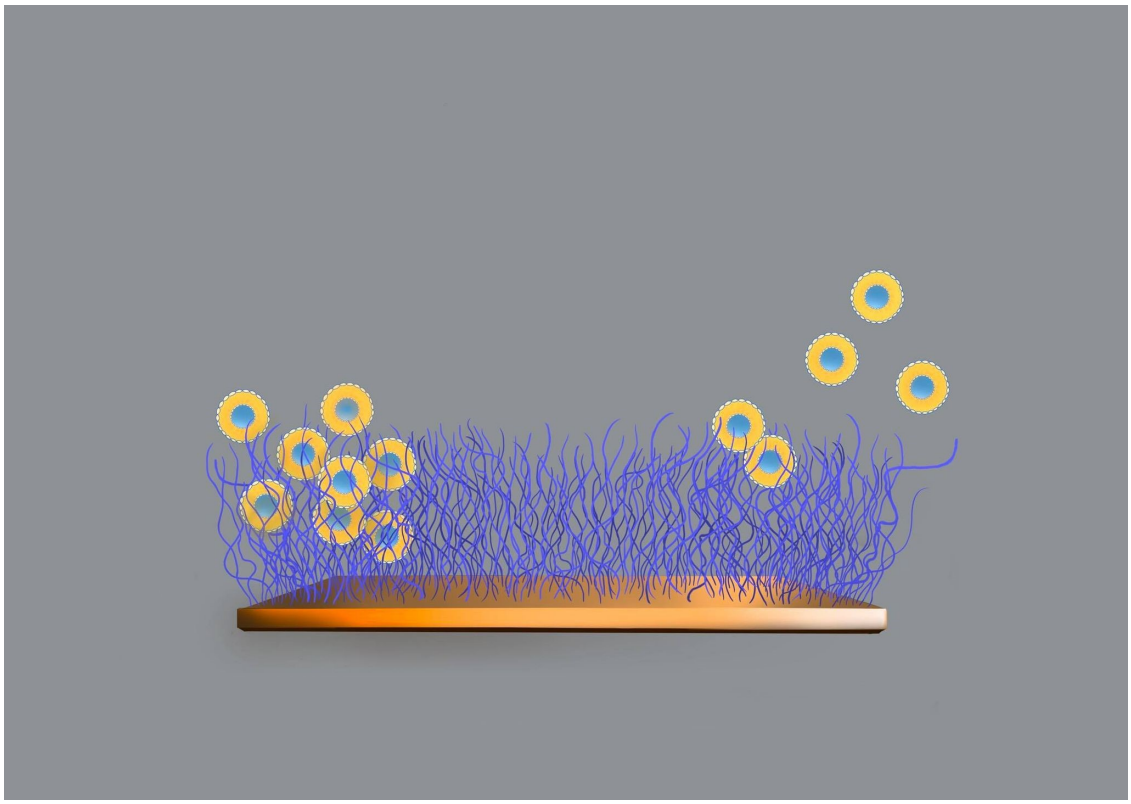

Electrochemical catch-and-release of biomolecules for development of new bio-electronic devices

Master's thesis in Materials Chemistry

Filip Cindric & Oliver Jacobsson Krstovic

DEPARTMENT OF CHEMISTRY AND CHEMICAL ENGINEERING

CHALMERS UNIVERSITY OF TECHNOLOGY
Gothenburg, Sweden 2022
www.chalmers.se

Master's thesis 2022

Electrochemical catch-and-release of biomolecules for development of new bioelectronic devices

Filip Cindric & Oliver Jacobsson Krstovic

CHALMERS
UNIVERSITY OF TECHNOLOGY

Department of Chemistry and Chemical Engineering
Division of Applied Chemistry
Chalmers University of Technology
Gothenburg, Sweden 2022

Electrochemical catch-and-release of
biomolecules for development of new bioelectronic devices
FILIP CINDRIC & OLIVER JACOBSSON KRSTOVIC

Supervisor: Gustav Ferrand-Drake del Castillo, Nyctea Technologies
Examiner: Andreas Dahlin, Department of Chemistry and Chemical Engineering

Master's Thesis 2022
Department of Chemistry and Chemical Engineering
Division of Applied Chemistry
Chalmers University of Technology
SE-412 96 Gothenburg
Telephone +46 31 772 1000

Cover: Biomolecules immobilised and release from a layer of polymer brushes.

Typeset in LaTeX
Printed by Chalmers Reproservice
Gothenburg, Sweden 2022

Electrochemical catch-and-release of biomolecules for development of new bioelectronic devices.

Filip Cindric & Oliver Jacobsson Krstovic
Department of Chemistry and Chemical Engineering
Chalmers University of Technology

Abstract

Purification is a key step when producing pharmaceuticals. A possible alternative to today's techniques, is by utilising weak polyelectrolyte brushes on an electrode surface. These have been proven successful regarding capture and on-demand release of biomolecules using electrochemistry. However, it has been difficult to achieve this at physiological pH. The reason is the repulsion that occurs between the brushes and the biomolecules. In this study, the brushes used are PAA and are negatively charged at physiological pH. Also, many biomolecules have low isoelectric points, making them negatively charged as well.

Two strategies will be evaluated to overcome the issue with capture and release at physiological pH. The first involves the polymer poly(L)lysine (PLL). PLL is cationic at physiological pH and is therefore expected to have an electrostatic attraction to the anionic brushes. Furthermore, it is possible to end-couple PLL in order to conjugate to the biomolecule of interest. The second strategy tests self-manufactured liposomes, where three different lipids will be tested. These are the zwitterionic lipid DPPC and the cationic lipids DOTAP and MVL5. The idea is that the formed cationic liposomes will electrostatically attract to the anionic brushes.

The capture and release of PLL was successful. Also, it is proved that lower molecular weight PLL is more suitable for the purpose than higher molecular weight PLL. Applied electrical potentials managed to partly release the PLL but to achieve complete release, a pH 2 solution was injected. At this state, the pH is far below pKa of the brushes and the electrostatic attraction is removed. For the second strategy, immobilisation was more challenging. Different liposome compositions were created, but only one managed to interact with the brushes at physiological pH. Furthermore, the release was incomplete even when different pH solutions were injected. The conclusion is that both of the strategies are worth to consider. However, further development is required to ensure capture and later release with electrochemistry, especially with the second strategy involving liposomes.

Keywords: polyelectrolyte brushes, electrochemistry, poly(L)lysine, liposomes, electrostatic attraction.

Acknowledgements

We would like to thank Andreas Dahlin and Maria Kiriakidou for their support and guidance during the project. Andreas, thank you for informing us about this master's thesis work and for the worthwhile discussions and Maria, thank you for the guidance in the laboratory.

Also, we would like to greatly thank Gustav Ferrand-Drake del Castillo for supervising this project. It was an honour to work with you and Nyctea during the spring. The football talks over a Mahogny coffee will be remembered.

Finally, we would like to thank family and friends for showing support throughout this spring.

Filip Cindric and Oliver Jacobsson Krstovic, Gothenburg, June 2022

List of Terms

Biology & physics

a	Monomer length (m)
b	Kuhn length (m)
c	Sauerbrey sensitivity constant (ng/cm^{2}Hz)
F	Fresnel coefficient
N	Number of monomers
n	Refractive index
f	Frequency (Hz)
m	Mass (g)
k	Wave vector (1/m)
k_b	Boltzman constant (m^{2}kg/s^{2}K)
pKa	Dissociation constant (acid)
pI	Isoelectric point
Q	Quality factor
R	Radius of polymer coil (m)
T	Temperature (K)
Γ	Grafting density
χ	Polymer-solvent parameter

Chemical names

DCM	Dichloromethane
DMSO	Dimethyl sulfoxide
DOTAP	Dioleoyl-3-trimethylammonium propane
DPPC	Dipalmitoylphosphatidylcholine
EtOH	Ethanol

MVL5	Multivalent cationic lipid
PAA	Poly(acrylic acid)
PBS	Phosphate-buffered saline
PLL	Poly(L)lysine
PMDETA	Pentamethyldiethylenetriamine
TBA	Tert-butyl acrylate
TBN	Tert-butyl nitrate

Analytical techniques

DLS	Dynamic light scattering
IR-RAS	Infra-red Reflective absorption spectroscopy
QCM-D	Quartz crystal microbalance with dissipation monitoring
SPR	Surface plasmon resonance

Contents

List of Figures

1
Introduction

The pharmaceutical industry is constantly under development with high demands. There are expectations on pharmaceuticals, such as over-time pain relief and low side-effects.[1] Furthermore, several parameters regarding pharmaceutical manufacturing have to be accounted for. Some examples are time for mass production and equipment cost, but in particular purification.[2] The time for production is of relevance since long manufacturing times, results in lower quantity of medicine that can help patients. When there is a high demand on pharmaceuticals, supply should not be a limitation. To ensure the supply, equipment that can produce the quantity is required. The scale-up is often expensive and therefore becomes a constraint for the production of pharmaceuticals.[3] Lastly, product purification is a parameter of high importance when it comes to pharmaceuticals. The effect of contamination in medicine can become fatal for the patient.[4]

Today, a common technique to purify pharmaceuticals is through affinity chromatography. In this technique, molecules are separated by interacting with the stationary phase. Why affinity chromatography sticks out from other chromatographic techniques, is because that the stationary phase contains specific receptors which has affinity for the molecules of interest.[5] In general, chromatography provides high purity products, but there are some downsides such as high equipment cost and difficulties to remove the separated compounds from the column.[6][7] By developing a new technique that solves these problems, pharmaceuticals would become cheaper and more available for the society. Furthermore, the production of them would require less raw material and benefit to the environment.

A possible solution, presented by Nyctea Technologies, is by utilising electrochemistry to selectively capture and release biomolecules. Biomolecules are substances produced by living cells, such as lipid nanoparticles or proteins, that can be charged depending on the surrounding pH. Furthermore, biomolecules are in a large extent used in pharmaceuticals.[8][9][10]

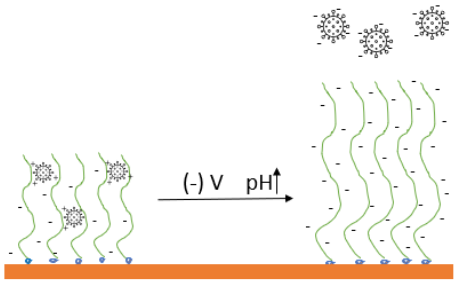

Figure 1.1: Weak polyelectrolyte brushes covalently attached to an electrode surface plate. Biomolecules are released since the local pH is increased by applying a negative potential.

The method employs a special type of polymer brush, so called weak polyelectrolyte brush. The advantage of these brushes is their ability to change their charge by altering the pH. This creates the possibility to adjust the electrostatic attraction between biomolecules and the brush. It enables capture by electrostatic attraction and release by electrostatic repulsion. An illustration of how the release could look like when an electrical potential is applied can be seen in Figure 1.1. The electrical potential induces, or consumes H^+, that will either decrease or increase the pH as long as the potential is applied.[11] Nyctea Technologies has proven that capture and release is possible when the bulk environment has pH 5, but has been found to be more challenging at physiological pH (pH $\sim$ 7) due to electrostatic repulsion.

1.1 Aim

The project aims to capture and release biomolecules from a surface on-demand at physiological pH. This will be performed using polyacrylic acid (PAA) as the anionic polyelectrolyte brush while poly(L)lysine (PLL) and cationic liposomes will be utilised as biomolecule carriers. The purpose of the biomolecule carriers is to electrostatically interact with the brushes as well as conjugate to the biomolecules of interest, at physiological pH. A successful implementation of biomolecule carriers would be helpful for the development and production of bioelectronic devices for biomolecule purification and drug delivery.

1.2 Limitations

The project focus will be on studying immobilisation of biomolecules on a certain type of brush. PAA brushes have been selected because they have a lower pKa than other common weak polyelectrolyte brushes, making them more charged at physiological pH. Furthermore, PLL and cationic liposomes have been selected as carriers since they are positively charged at physiological pH. Solid lipid nanoparticles is another interesting carrier molecule, but was not tested due to a limited time frame.

2
Theory

The principles that enable capture and release are presented in this section. This involves basic knowledge about polymer brushes and possible interactions with each other and the surrounding, as well as manufacturing methods. Furthermore, the two strategies and how the carriers interact with the polymer brushes are explained. The main characterisation techniques to study the polymer brushes and how they interact with biomolecules are surface plasmon resonance and quartz crystal microbalance with dissipation monitoring, and will be declared in this section.

2.1 Polymer brushes

When one end of a polymer chain is covalently attached to a surface, a polymer brush is formed. Polymer brushes can alter the surface properties depending on the application.[12] For instance, immobilisation of different molecules or repulsion of them from the surface.

To understand the principles of polymer brushes, the behaviour of polymers in a solvent has to be discussed. The total free energy, G(r), of a polymer in a solvent is dependent on the excluded volume, configurational entropy and interaction between the polymer chain and the solvent. The relation is presented in Equation 2.1 where r is the radius of a polymer coil, χ is the polymer-solvent parameter, N is number of monomers, a is the monomer size and b is the Kuhn length. Also, v is the volume of the monomer. [11][13]

$$G(r) = \frac{3k_bTr^2}{2abN} + \frac{k_bTvN^2}{r^3} - \frac{k_bTvN^2\chi}{r^3} + constant \tag{2.1}$$

The first part of the equation is the configurational entropy, where G(r) increases with larger r. For larger r, it becomes harder for the polymer to take on many configurations.[11] However, the excluded volume also affects G(r). In this case, it is favourable for the polymer chain to expand and take up more volume, lowering G(r). This counteracts the configurational entropy, where increased r increases G(r). The last part is the interaction between the solvent and the polymer coil. One essential parameter to describe this, as well as the equilibrium size of the polymer coil, is χ. If $\chi < 1$, the polymer chain and solvent attract each other, and $R \propto N^{3/5}$. The coil and the solvent repel each other at $\chi > 1$, and $R \propto N^{1/3}$. In a solvent where $\chi = 1$, the excluded volume and the interaction compensate each other and cancel out

while $R \propto N^{1/2}$.[11][13]

In a similar way as previously explained, the free energy of a polymer in a brush can be estimated but based on its height instead. By deriving the equation, together with assumptions and minimisation of the free energy, the height h of a polymer brush can be determined.[11][13]

$$h = (\frac{abv\Gamma}{3})^{1/3} * N \tag{2.2}$$

As showed in Equation 2.2, the height of a polymer brush is dependent on the number of monomers as well as the grafting density Γ. Γ corresponds to amount of polymer chains per unit area, and is influenced by the method of forming them. They can either be formed by a grafting-from or grafting-to method. In grafting-from, brushes are grown from the surface using initiators. This often generates higher Γ compared to grafting-to method, where the premade brushes are attached to the surface.[14] An illustration of the methods can be seen in Figure 2.1.

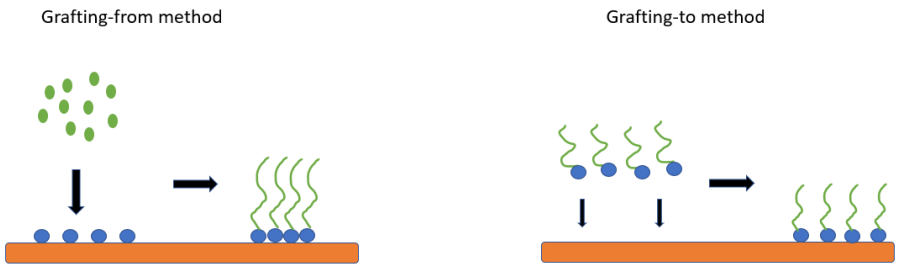

Figure 2.1: Grafting-to and grafting-from attachment on metal surface.

Besides the height of the brush, Γ also affects the conformation. For lower Γ, the polymer take on a so called mushroom shape. At this state, the height of the brush is similar to a polymer coil in a solvent. In other words, the chains are not stretched and it becomes difficult to immobilise large amounts of biomolecules in many layers.[11]

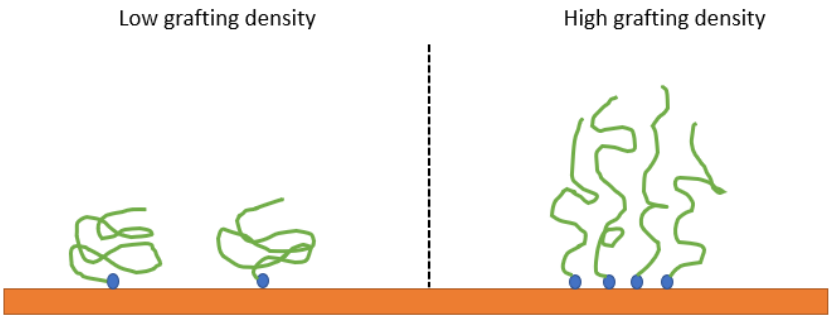

Figure 2.2: Illustration of low versus high grafting densities of polymers on a surface.

For larger Γ, the brushes will spontaneously stretch due to repulsion between them. This will ensure that the biomolecules interact with the brushes, and not the surface where the brushes are grafted on.[11] The two situations are illustrated in Figure 2.2. However, for immobilisation to occur, there also has to be an interaction between the polymer brushes and biomolecules.

2.1.1 Polyelectrolyte brushes

When a polymer brush carries charged functional groups, it is referred to a polyelectrolyte brush. A charged brush attracts counter-ions due to the electrostatic interactions between them, see Figure 2.3. Furthermore, a charged brush becomes more hydrophilic and will couple water. Thereby, swelling of the brushes occur.[11][15][16]

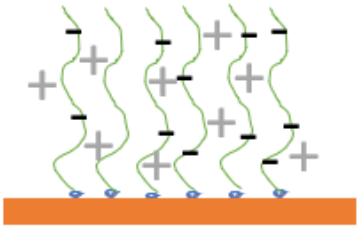

Figure 2.3: Polymer brush layer with charge compensations on a planar surface.

There are two types of polyelectrolyte brushes. Weak polyelectrolyte brushes are pH responsive, because of their functional groups being either weak acids or bases. The second type is strong polyelectrolyte brushes, where the functional groups are permanently charged and are not affected by the pH of the solution.[17] In the case of a weak polyelectrolyte brush, the pKa of the functional groups will determine the protonation state of the brush. When the surrounding pH is less than pKa, the functional groups remain protonated and the other way around, pH > pKa, the functional groups dissociate.[11]

In this study, polyacrylic acid (PAA) is used as polyelectrolyte brush, formed via atom transfer radical polymerisation (ATRP).[18] PAA is a weak anionic polyelectrolyte with pKa around 5.6 at physiological salt content 150 mM NaCl.[19][20] A sketch of the chemical structure in protonated and deprotonated state can be seen in Figure 2.4.

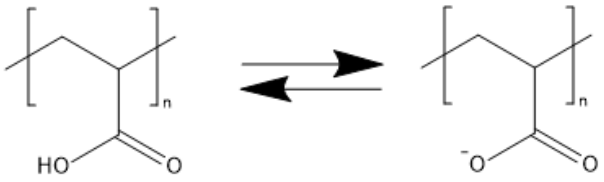

Figure 2.4: The carboxyl group on PAA becomes negatively charged when pH is increased above pKa.

2.1.1.1 Biomolecule and brush interaction

For the biomolecules to interact with the anionic brushes, there has to be an attraction which can be achieved in two ways.[21] The first one is through electrostatic attraction and only occurs if the biomolecules have opposite charge to the brushes. The charge depends on the isoelectric point, pI, which corresponds to at what pH the net charge of the biomolecules is zero. This results in two cases;[22]

- pI > pH, the biomolecules are positively charged.
- pI < pH, the biomolecules are negatively charged.

This indicates that biomolecules with pI > pH can interact with the anionic brushes, assumed that pH > pKa. To later remove this electrostatic attraction and thereby release the biomolecules, pH can be changed. By increasing pH above both pI and pKa, the net charge of the biomolecules will change and repulsion occurs.[11]

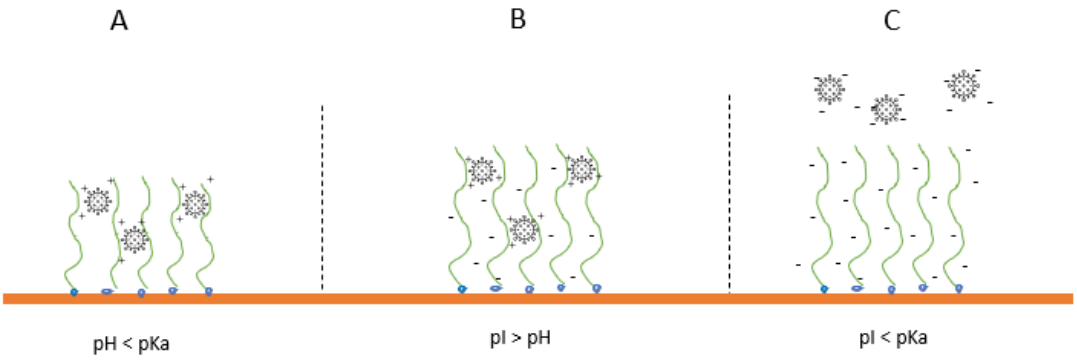

Figure 2.5: Brush interactions for biomolecules to PAA brushes. Capture is possible via hydrogen bonding (A) and electrostatic interactions (B). Capture is not possible of biomolecules with pI < pKa (C). For case B and C, pH is assumed to be above pKa.

However, since there are several different functional groups on a biomolecule, interaction through hydrogen bonding may also occur. This interaction is not well established, but earlier studies have documented that there is an interaction between protonated poly(carboxylic acid) brushes and certain biomolecules, such as

proteins.[21] It can be removed by creating repulsion between the brushes and the biomolecules. This is achieved by increasing the pH above the pKa of the brushes and pI of the biomolecules.[11] Figure 2.5 shows how binding occurs with hydrogen bonds (A) and electrostatic attraction (B), as well as release with electrostatic repulsion (C) when pI < pKa.

2.2 Immobilisation of biomolecules at physiological pH

PAA is negatively charged at physiological pH. To successfully bind biomolecules with pI < physiological pH, two different strategies will be tested. The first one is by conjugating biomolecules to poly(L)lysine (PLL) and the second is by utilising liposomes.

2.2.1 Poly(L)lysine

The first strategy is to use PLL as biomolecule carrier. PLL is a binder polymer with a pKa around 10, making it positively charged at physiological pH.[23] Due to its pH responsiveness and biocompatibility, PLL is often used in applications involving drug delivery.[24] The structure is presented in Figure 2.6.

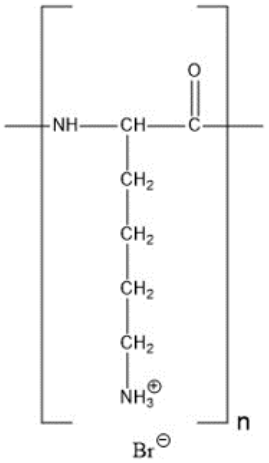

Figure 2.6: Chemical structure of PLL.

PLL can interact by electrostatic attraction to anionic molecules, such as PAA. However, it must also be able to conjugate to the biomolecule. This can be done by attaching a molecule to the end of the PLL chain, in order to attract a biomolecule of interest.[25]

In this study, PLL with end-coupled biotin will be tested. Biotin has strong affinity for the biomolecule avidin, or its analogues streptavidin and neutravidin. Avidin has four binding sites and the interaction with biotin is strong, non-covalent and specific.[25][26]

2.2.2 Liposomes

A common procedure to have a safe and biocompatible drug delivery is by utilising a certain type of lipid nanoparticle, called liposomes.[27] As showed in Figure 2.7, liposomes are small vesicles, composed of phospholipids with a structure that exhibits both hydrophobic and hydrophilic behavior. This is possible due to the bilayer with a closed compartment inside where the active substance can be present. The hydrophilic head groups of one layer points to the interior and the other one to the bulk. This enables the carrier ability, which can be used for various pharmaceutical and cosmetic applications.[28]

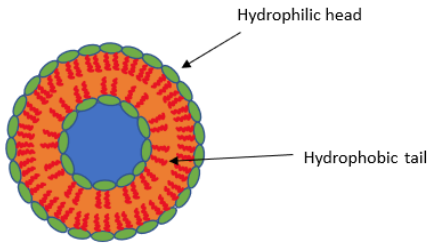

Figure 2.7: A liposome where the lipids form a bilayer. The lipids consists of hydrophobic tails and hydrophilic head groups.

Liposomes can be neutral, cationic or anionic depending on the lipids, and can be produced with an extrusion procedure. Three different pH-responsive lipids will be tested in different amounts, DPPC, DOTAP and MVL5. DPPC is a zwitterionic lipid which means that it contains both positively and negatively charged groups, while the other two are cationic.[29][30] Their chemical structures can be seen in Figure 2.8.

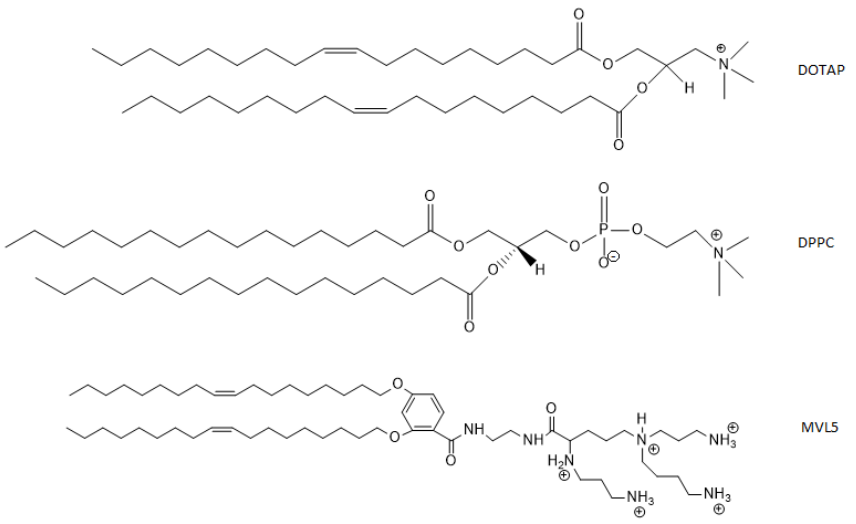

Figure 2.8: Structures of the tested lipids.

DPPC will be mixed with either DOTAP or MVL5 to create cationic liposomes. The purpose is to electrostatically attract to the negatively charged brushes. Due to mixing of lipids at different compositions, its difficult to estimate the pKa of the liposomes without measuring it. However, the liposomes will be positively charged at physiological pH since cationic lipids are used.

2.3 Local pH alteration using electrochemistry

One way to release the captured biomolecules is by applying electrical potentials. When a potential is applied, a pH gradient at the surface is generated and lasts as long as the potential is applied. Depending on whether the potential is positive or negative, different reactions will occur.[11] For the case below, a negative potential will reduce O_2 to H_2O and H_2O_2.[31]

$$O_2 + 4H^+ + 4e^- \longrightarrow 2H_2O$$

$$O_2 + 2H^+ + 2e^- \longrightarrow H_2O_2$$

The consumption of protons lead to an increase in local pH and a pH gradient is created. At physiological pH, the PAA brushes will be negatively charged. To protonate the PAA brushes from a deprotonated state, a reducing agent is necessary due to the difficulties to oxidise H_2O. The reducing agent will therefore serve as a proton supplier to the system, when a positive potential is applied.[11]

2.4 A system for capture and release of biomolecules at physiological pH

To have a successful capture and release of biomolecules at physiological pH, several parts have to be considered. As previously mentioned, grafting density Γ plays a key role to make capture possible. Large Γ is achievable using grafting-from as method of forming the brushes.

Another requirement to immobilise biomolecules is that they have to interact with the brushes at physiological pH and later be released, on-demand. Weak polyelectrolyte brushes can be utilised for this purpose, due to their ability to be charged and non-charged depending on the pH. PAA is a suitable polyelectrolyte due to the ability to electrostatically attract biomolecules at physiological pH. However, many biomolecules have low isoelectric points. As a consequence, repulsion from the PAA brushes will occur since both the brushes and the biomolecules are negatively charged at physiological pH. Therefore, PLL and liposomes will be used as carriers of the biomolecules, allowing them to be captured and later released.

The electrochemical release of the carriers is triggered by changing the local pH. By applying an electrical signal, a pH gradient is created on the surface of the electrode. This will change the protonation state of the functional groups on the brushes, making the electrostatic attraction repulsive and the carriers are released.

2.5 Characterisation methods

There are several techniques that can be used to investigate how well the carriers interact with the polyelectrolyte brushes. The two main techniques in this study are surface plasmon resonance and quartz crystal microbalance with dissipation monitoring. There are complementary techniques such as dynamic light scattering, to ensure that liposomes with correct diameter were produced and infra-red spectroscopy, to verify that the carriers bound to the brushes and that the synthesis of the brushes was successful. However, they are not used to investigate the interaction in real-time and are therefore not declared in this section.

2.5.1 Surface Plasmon Resonance

A method to confirm a reversible interaction between molecules is by utilising surface plasmon resonance (SPR). The interaction is studied via surface plasmons, which are produced between a metal and a dielectric material when electrons along the interface are excited by light. This will cause them to oscillate and thereby create an electromagnetic field, whose amplitude gets reduced further away from the interface.[11][32][33] Figure 2.9 shows how the wave travels along the interface.

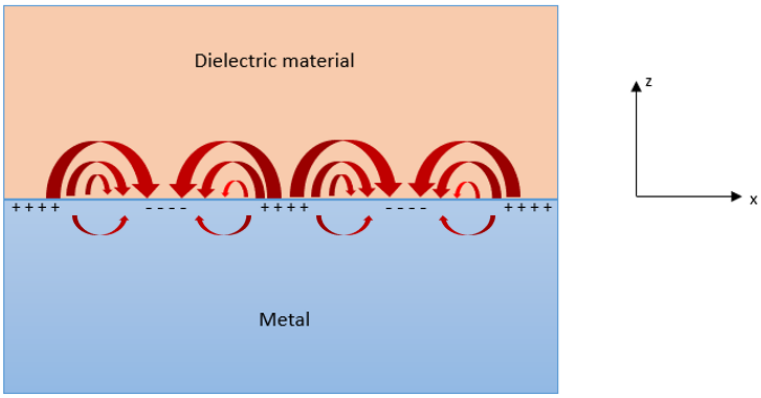

Figure 2.9: The wave on a surface. The further into the dielectric material (in z-direction), the weaker electrical field.

The excitation of electrons occur when a light beam interferes with the interface at a certain angle, the so called SPR-angle and can be observed as a minimum in reflectivity in a SPR-curve. An illustration of such a curve is presented in Figure 2.10.

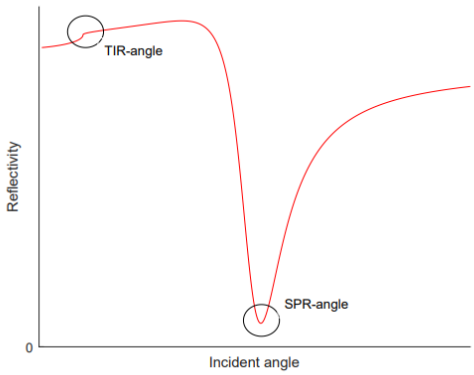

Figure 2.10: A SPR measurement where a light beam is passed through a goniometer, penetrates the prism on the surface and later hits the surface at different incident angles. A detector registers the reflectivity for each angle. From the curve, TIR and SPR-angle can be determined.

When the refractive index changes on the surface, for example when a molecule approaches it, a shift in SPR-angle is observed. This shift does not tell whether the surface or the bulk refractive index was changed. To enable estimation of only the surface refractive index, TIR-angle has to be accounted for. Total internal reflection, or TIR, tells the refractive index of the bulk.[11] The refractive index can be estimated on the basis of Snell's law:

$$n_1 sin(\theta_i) = n_2 sin(\theta_r) \tag{2.3}$$

where n_1 is the refractive index of the prism on the surface and n_2 is the bulk refractive index. θ_i and θ_r corresponds to incident and transmitted angle of the light. At a certain incident angle, θ_r becomes 90° and the refractive index of the bulk can be calculated.[11][34]

2.5.1.1 Dry height estimation by Fresnel modelling

The reflectivity from the spectrum enables estimation of the dry height of polyelectrolyte brushes. This is done by fitting a model to the actual reflectivity-incident angle curve from the measurement, called Fresnel modelling. Compared to the case with Snell's law, Fresnel modelling takes layer thicknesses into account. Depending on the SPR reflectivity from the measurement, the Fresnel model is fitted to match the measurement, using literature values for refractive indices and known thickness of the metal film. This creates the possibility to calculate the unknown thickness of a layer.[11][35]

To study the amount of light that is reflected or transmitted through the surface, Fresnel coefficients are used that describe the amount of light for each case. The coefficients have values between 0 and 1, depending how the light interferes with the surface.[11][33] The Fresnel equations are presented below.

$$F_r = \frac{F_{r,12} + F_{r,23} e^{i2k_0 d n_2 cos(\theta_2)}}{1 + F_{r,12} F_{r,23} e^{i2k_0 d n_2 cos(\theta_2)}} \tag{2.4}$$

$$F_t = \frac{F_{t,12} + F_{t,23} e^{i2k_0 d n_2 cos(\theta_2)}}{1 + F_{t,12} F_{t,23} e^{i2k_0 d n_2 cos(\theta_2)}} \tag{2.5}$$

The situation described above is illustrated in Figure 2.11, where F_r is the Fresnel coefficient for the reflected light and F_t is the corresponding for transmitted light.

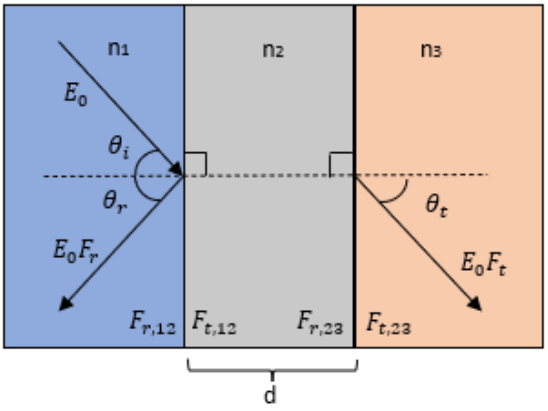

Figure 2.11: Three materials with different refractive indices, two interfaces and one layer. E_0 is the incident electric field and d is the layer thickness.

In this study, more than one layer is involved. To observe the complete reflection or transmission of light through the interfaces when more than one layer is present, a

transformation matrix Φ is used and is described in Appendix A.2.[33]

Fresnel modelling demands several parameters, such as refractive indices and thicknesses. When these are known, it is a tool to estimate the unknown thickness of a layer, for example the dry height of polyelectrolyte brushes. Furthermore, besides providing a SPR-curve for dry height, liquid measurements can be performed. In these experiments, the SPR-angle responds to when something attaches to the polyelectrolyte brushes or is removed from them. This is one technique to investigate the capture and release of biomolecules, but a complementary technique for this task is QCM-D.

2.5.2 Quartz crystal microbalance with dissipation

Quartz crystal microbalance with dissipation monitoring (QCM-D) is a surface sensitive technique to study changes in mass at the surface in real time. The QCM-D consist of a piezoelectric material called a quartz crystal sensor.[36] When a varied electric potential is applied, the generated electric field causes the quartz crystal to move. Following, it starts to oscillate at a specific resonance frequency when the electrical potential is removed. The frequency will shift when mass is added or removed from the quartz crystal, which can be described by the Sauerbrey relation presented in Equation 2.6.[11]

$$\Delta m = \frac{C}{n}\Delta f \tag{2.6}$$

C is the sensitivity factor and n is the overtone number. Δm corresponds to the change in mass while Δf is the observed frequency shift.[37] However, this relation is only valid if the mass adsorbed is small compared to the quartz crystal weight, well distributed over the entire surface and that the adsorbed mass is rigid.[38] Since polyelectrolyte brushes are flexible and swell when in contact with a good solvent, this relation is not valid for those measurements. Instead, polyelectrolyte brushes can be described as a viscoelastic film. Therefore, both the change in energy dissipation and frequency has to be considered when polyelectrolyte brushes are utilised. The decrease in dissipation due to its swelling and flexibility can be explained by the relation below, where Q is the quality factor.[11][37]

$$D = \frac{1}{Q} = \frac{E_{dissipation}}{2\pi E_{stored}} \tag{2.7}$$

However, one advantage with the QCM-D is that the dissipation can be measured along with the frequency. By fitting the measured oscillation to a exponentially decaying oscillation, dissipation can be calculated. τ is the decaying time constant and is expressed together with the frequency in the equation below.[37]

$$D = \frac{1}{\pi f \tau} \tag{2.8}$$

QCM-D can be used to study capture and release of biomolecules with electrochemistry. By connecting a potentiostat to the flow cell, electrical potentials can be applied to the quartz crystal sensor.

2.5.2.1 Electrochemical release with QCM-D

The charged state of the polyelectrolyte brushes will change depending on the local pH. By utilising electrochemistry with QCM-D, structural variations of the brushes can be studied in real time.[39] Also, on-demand release of biomolecules from the brushes can be observed. The setup is illustrated in Figure 2.12. A potentiostat is used to send either a positive or negative electrical potential to the sensor.[11]

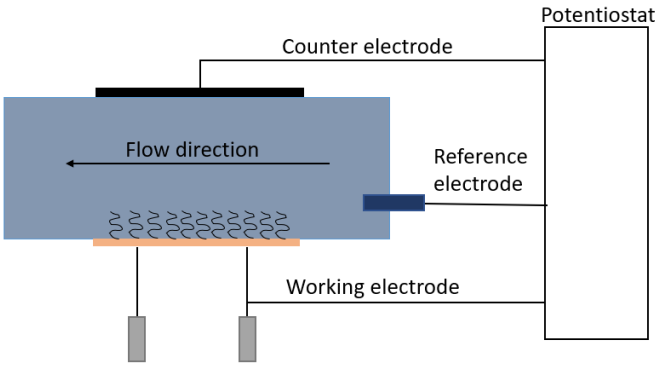

Figure 2.12: Simplified illustration of a potentiostat connected to the QCM-D. At the top, there is a Pt ceiling in contact with the electrolyte solution flowing through the system. The reference is connected to a outlet close to the QCM-D sensor where the working electrode is. Below the QCM-D sensor are measurement pins from where the current can pass through.

The potentiostat is connected via a counter, reference and working electrode where the reference measures the voltage and should show a constant potential while its applied.[11][39][40]

3
Methods

3.1 Laboratory Work

The weak polyelectrolyte brushes that will be utilised are PAA. These will be grafted to QCM-D and SPR sensors. All the chemicals used are presented in Appendix A.1.

3.1.1 Synthesis of diazonium salt

In advance to the synthesis of diazonium salt, 200ml of diethyl ether was poured in a beaker and placed in the freezer. For the synthesis, a 25ml flask and a vial were cleaned with EtOH and dried with nitrogen (N_2). In the following order, 2.942g aminophenetyl alcohol, 12ml of acetonitrile and 7.2ml tetrafluoroboric acid were added to the 25ml flask. In the vial, 12ml acetonitrile and 2.626ml tert-butylnitrate were added. Both the vial and the flask were degassed for 20 minutes and were then placed in the freezer for 2 hours.

After the 2 hours, the vial was placed in a ice bucket and the flask was put in a second ice bucket, and placed on a stirrer. With a glass pipette, the solution in the vial was added drop by drop into the flask. When the solution was transferred, the flask was degassed and stirred for 1 hour. When the degassing of the flask was completed, the diethyl ether prepared in advance was put in a new ice bucket and the degassed solution was transferred with a glass pipette into the diethyl ether.

The new solution is not stable in room temperature and was therefore placed in the freezer over night. The last step was to transfer the produced diazonium salt (solid phase) to a new vial with a glass pipette.

3.1.2 Synthesis of PAA

PAA brushes were produced on the sensors according to the following reaction scheme.

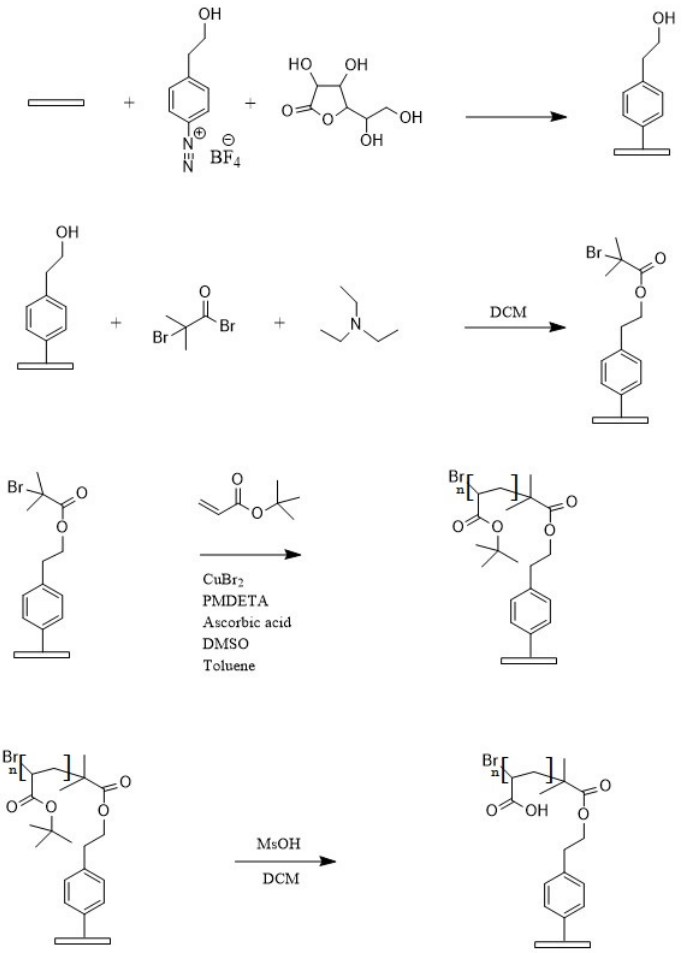

Figure 3.1: Reactions during the synthesis of PAA brushes

L-ascorbic acid and diazonium salt put ground for the build up of the brush. Initially, the sensors were cleaned with EtOH and Milli-Q water followed by drying with N_2. To a vial, 0.028g L-ascorbic acid was added together with 40ml Milli-Q water and was left to degas for 1 hour. Meanwhile, additional cleaning of the sensors was performed. In the first cleaning step, 30ml sulfuric acid and 10ml hydrogen peroxide were mixed in a beaker. The stand with the surfaces was placed inside for 20 minutes. The stand was put in a beaker of Milli-Q water. The surfaces were, one by one, rinsed with Milli-Q water, EtOH and dried with N_2. In the second cleaning step, 30ml Milli-Q water, 6ml ammonium hydroxide and 6ml hydrogen peroxide were mixed in a beaker and the stand with the surfaces was placed inside. It was left for 20 minutes at 120°C. The surfaces were then rinsed as in the first step.

In a beaker with the surfaces on a new stand, 0.30g of unfrozen diazonium salt was added together with the degassed L-ascorbic acid and a stir magnet. The beaker was left on a mixing plate for 80 minutes. After 40 minutes, two round flasks were

prepared with different solutions. In the first, 8mg copper(II)bromide , 25ml DMSO, 0.056ml PMDETA, 8.5ml TBA and 11ml toluene were mixed and left to degas for 1 hour. In the second, 65mg L-ascorbic acid and 1.5ml DMSO were mixed and left to degas for 4 minutes.

After 80 minutes, the surfaces were taken out from the diazonium salt and L-ascorbic acid mixture, rinsed with EtOH and dried with N_2. The stand was placed in a clean jar with EtOH. To replace the hydroxyl group with a bromide, 0.222mL $\alpha-$bromoisobutylbromide, 20ml DCM and 0.3mL triethylamine were added to the jar. The beaker was plate stirred for 10 minutes. Afterwards, the surfaces were withdrawn one by one and later rinsed with EtOH, dried with N_2 and placed on a clean stand.

When the round flasks degassing were completed, the clean stand with the surfaces was put in a clean jar with a stirring magnet. All liquid from the first degassed round flask was transferred to the jar. From the second degassed round flask, 1ml of the mixture was poured into the jar. The jar was properly sealed and left to stir over night at 500rpm. Afterwards, the stand was placed in a clean jar with 99% EtOH. The surfaces were withdrawn one by one, rinsed with EtOH and dried with N_2. To a new beaker, 15mL of DCM and 100mL of methanesulfonic acid were added. The stand was placed inside the beaker and left to stir for 15 minutes. Lastly, the surfaces were thoroughly rinsed with EtOH and dried with N_2 before placed in holders.

3.1.3 Liposome manufacturing

Cationic liposomes were produced with Avanti® Mini Extruder. Initially, a 50ml flask was rinsed EtOH and dried with N_2. The lipids were mixed with chloroform in the flask and was connected to a rotary evaporator for 45 minutes. The concentration of lipids were prepared to range between 10-15mg/ml. Furthermore, the chloroform was added via a glass pipette to avoid contamination. While the rotary evaporator was running, the retainer nuts and syringes were cleaned with EtOH and Milli-Q, and the extruder outer casing cleaned with EtOH. A PBS buffer of pH 7.4 was also prepared.

After the 45 minutes, a thin lipid film was observed on the bottom of the flask. To dissolve this, 1.5ml of PBS buffer was added to the flask and parafilm was placed on top of it to seal it. The flask was left to sonicate for 20 minutes.

The mini extruder set up was prepared according to Avanti® protocol and one of the syringes was filled up with the solution from the flask. The syringes were connected to the extruder outer casing and attached to a heating block with a temperature of 55-60°C. Heating was used to facilitate extrusion. The solution was pressed from one syringe to the other, through a 100nm filter in the extruder for 21 times. The extruder outer casing was removed from the heating block and the 100nm filter was replaced with a 50nm filter. Extrusion took place for 21 times again, at 55-60°C.

To verify that the liposomes were successfully produced, dynamic light scattering (DLS) measurements were performed. The instrument measures the size and size distribution of the liposomes. To find the best method for creating liposomes, many DLS measurements were performed.

3.2 Angular spectroscopy with SPR

Polyelectrolyte brushes were according to previously mentioned protocols grafted to SPR sensors. Before placed in SPR holder, one sensor was cleaned with EtOH, gently dried over a paper, cleaned with EtOH once again and then dried with N_2. The sensor was placed in the SPR holder, inserted into the machine and a dry scan was performed. The angle-reflectivity graph was used together with Fresnel modeling to determine the dry height of the polymer brushes. For the continuous liquid measurement scan, a well-plate was prepared with the solutions. The SPR was later programmed to inject the solution at a certain interval. For every measurement was a post-delay timer of 5 minutes set to allow PBS buffer flow through the system.

3.3 Mass measurement using QCM-D

Initially, the instruments components were rinsed with EtOH, Milli-Q water and dried with N_2. This involved the cell as well as hoses and clamps. The QCM-D sensor, with the polyelectrolyte brushes grafted on, was also rinsed in the same manner. Before the measurement, the cell was prepared with a reference electrode, an inlet hose from the sample and an outlet hose running through a pump and later to waste. The pump was used to control the flow rate of the liquid. Besides these, cables that connects the cell with the potentiostat were inserted.

In the initial part of the measurements, a baseline was set. Afterwards, the inlet was switched to a buffer solution, without biomolecules, with pH equal to the one in the solution containing the biomolecule. Before switching inlet to the biomolecule solution, the pump was paused and the hose was transferred quickly to prevent air bubbles from appearing. The flow rate of the liquid in the system was set to 0.150µL/min. The biomolecules were immobilised in the polymer brush and to remove the biomolecules from the brushes, a voltage was applied. The voltage applied was increased until the biomolecules were released, at a maximum of -1V or +1V.

4

Results and discussion

This chapter is divided into three sections. Initially, PLL is captured and released. Afterwards, PLL-biotin interaction with the brushes is studied and lastly, liposomes are examined. All performed measurements were executed at physiological pH unless otherwise stated. The dry height of the brushes used in the experiments varied between 25-50nm, and an example of a Fresnel estimation is illustrated in Figure A.1 in Appendix A.2.

4.1 Capture and release of PLL

The interaction between PLL (30 000-70 000 g/mol) and PAA at physiological pH was studied using SPR, QCM-D and IR. After each immobilisation, the systems were rinsed with buffer at physiological pH, seen as the non-coloured areas in the upcoming figures.

From the SPR measurement, it can be seen that the angle shift increased when PLL was injected, see Figure 4.1. The shift in angle is a consequence from a change of refractive index which happens when PLL interacts with the brushes. To release PLL, both increase and decrease in pH were tested. As previously described, PLL has a pKa of 10 which indicates that the increase in pH is expected to remove the electrostatic interaction between PLL and the brushes. However, the release was not accomplished and one reason might be that there still are some charges left on PLL that can interact with the brushes. Increasing the pH higher than pH 11 might have worked, but since pH 2 managed to release, this was not tested.

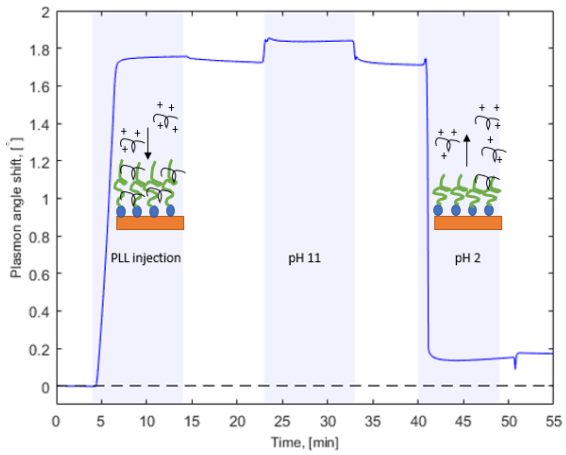

Figure 4.1: PLL is captured onto the brushes, causing an increase in angle shift. It is not released when injecting a solution with pH 11. However, at pH 2, the electrostatic attraction between PLL and the brushes is removed which results in a release of PLL.

Almost complete release of PLL was achieved at pH 2, see Figure 4.1. The most likely explanation is that the brushes are almost fully protonated at that pH, removing the electrostatic attraction. To verify that PLL had interacted with the brushes, IR measurements were performed. The result confirms that binding occurs and the spectrums with the characteristic peaks are presented in Appendix A.5.

To study the brush behaviour when PLL interacted with the brushes, QCM-D measurements were performed and the outcome can be seen in Figure 4.2. The initial pH switch of the experiment verifies the responsiveness of the brushes. By switching to pH 5, the brushes becomes more protonated. Increased amount of protonated groups makes the brushes more hydrophobic and will therefore swell less. In other words, the frequency increases and dissipation decreases since less water is present within the brushes.

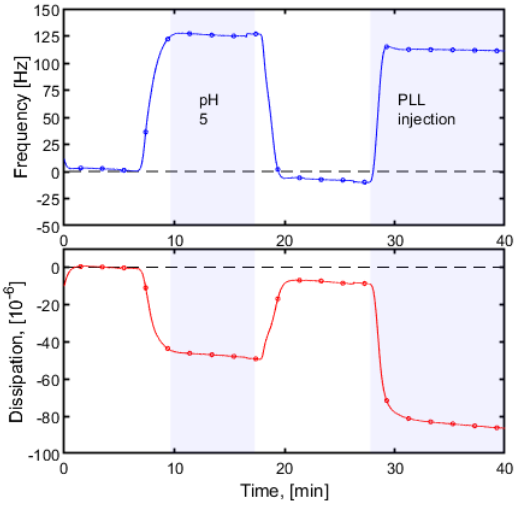

Figure 4.2: QCM-D measurement where pH 5 confirms brush responsiveness and later injection of PLL.

At the time when PLL is injected, the frequency starts to increase again. This is the opposite from what was expected, since added mass should decrease the frequency. One explanation might be that PLL has a large molecular weight. The larger molecular weight, the more possibilities for binding to occur which seems to result in brush collapse. Before PLL approaches, the brushes are highly hydrophilic and will couple great amounts of water. As soon as PLL is injected, it will start to compete with water over the brushes. Since the PLL has a large molecular weight, it will leave less space for water to interact. As a consequence, a significant amount of water is removed and the brush layer will become more compact and rigid. This is observed as a large decrease in dissipation in Figure 4.2. Furthermore, from the frequency increase, one can assume that the PLL layer weigh less than the previously coupled water. To successfully bind PLL without collapsing the brush, PLL with a lower and more narrow molecular weight distribution is tested.

4.1.1 PLL-biotin interaction with PAA

Lower molecular weight PLL (3300 g/mol) with end-coupled biotin was tested in the same manner as before with QCM-D. This time, a large frequency decrease is observed when PLL-biotin was injected. As compared to the larger molecular weight PLL, a smaller amount of water is probably removed and brush collapse is therefore avoided. Figure 4.3 illustrates a successful binding at physiological pH and release at pH 2.

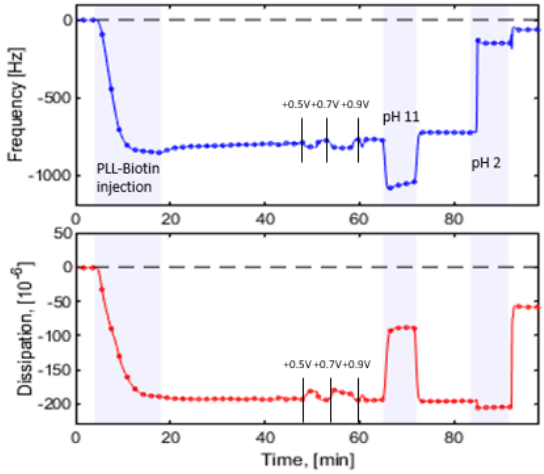

Figure 4.3: PLL-biotin injection and an attempt to release by applying three different electrical potentials. Almost complete release occurred at pH 2.

Previous measurements with PLL proved release at pH 2, hence positive potentials were applied with hydroquinone as reducing agent. This is another way to cause a decrease in pH and the potentials applied were +0.5V and +0.7V for 180s, but also +0.9V for 30s. As can be seen in Figure 4.3, no significant amount of PLL-biotin was released from the applied potentials. The release was more difficult compared to another performed experiment where a biomolecule named BSA was released with applied electrical potentials, see Appendix A.3. One possible explanation to the difficulties to release may be that the PLL-biotin and PAA interaction is stronger than for the case with BSA. Something to bring to this discussion is that the BSA experiment was performed at pH 5, where the brushes are less charged. Therefore, the attraction may be weaker and release becomes easier compared to PLL-biotin.

However, PLL-biotin is successfully released at pH 2. The applied potentials are therefore probably not able to create the corresponding local pH. The reason why even higher potentials were not applied is because it damages the surface, including the brushes. Further, to accomplish release with electrochemistry, parameters such as mass transport, flow rate and time of applied potentials may have to be considered.

Since PLL-biotin can be captured and released by switching pH, experiments involving neutravidin were performed. Neutravidin is a protein with low pI and did not interact with the brushes at physiological pH, see Figure 4.4.

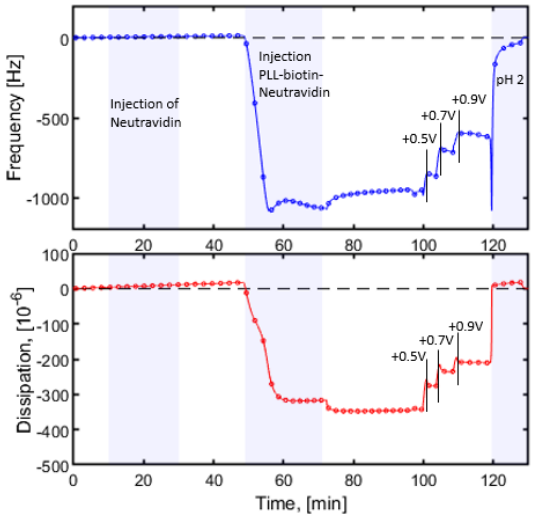

Figure 4.4: Initially, neutravidin was injected alone and did not interact with the brushes. Following, PLL-biotin-neutravidin complexes were injected and released by applying electrical potentials. All of the complexes did not release though, hence pH 2 was injected.

20 minutes before injection, neutravidin and PLL-biotin in a 1:4 molar ratio were mixed. The interaction between biotin and neutravidin is well studied and is therefore assumed to happen. Injection of the mixture resulted in binding, observed as a negative frequency shift. To trigger the release, potentials of +0.5V and +0.7V were applied for 180s and +0.9V for 30s. One can observe that some of the PLL-biotin-neutravidin complexes were released, since the frequency shift increased 400Hz. For complete release, pH 2 was as in previous experiments injected. It appears that the complexes were more easily released with electrochemistry compared to only PLL-biotin. This might be due to neutravidin reducing the number of conformations for PLL-biotin to adopt. PLL is a polymer that can orient to achieve the most optimal interaction with the brushes. When PLL-biotin attaches to neutravidin, the number of conformations decreases which ends up in fewer ways to interact. This will weaken the interaction with the brushes and release can occur more easily.

For further improvements of the complex interaction with the brushes, even lower molecular weight PLL-biotin can be tested. Due to fewer lysine groups, these complexes will have weaker attraction to the brushes, which is an advantage regarding release with electrical potentials.

4.2 Capture and release of liposomes

The second carrier to study was liposomes. Since the lifetime for liposomes is expected to range between 3-5 days, new formulations had to be done regularly. To verify the sizes of the produced liposomes, as well as their size distributions, dynamic light scattering (DLS) measurements were performed. Figure 4.5 illustrates an example of how the result from DLS looks like.

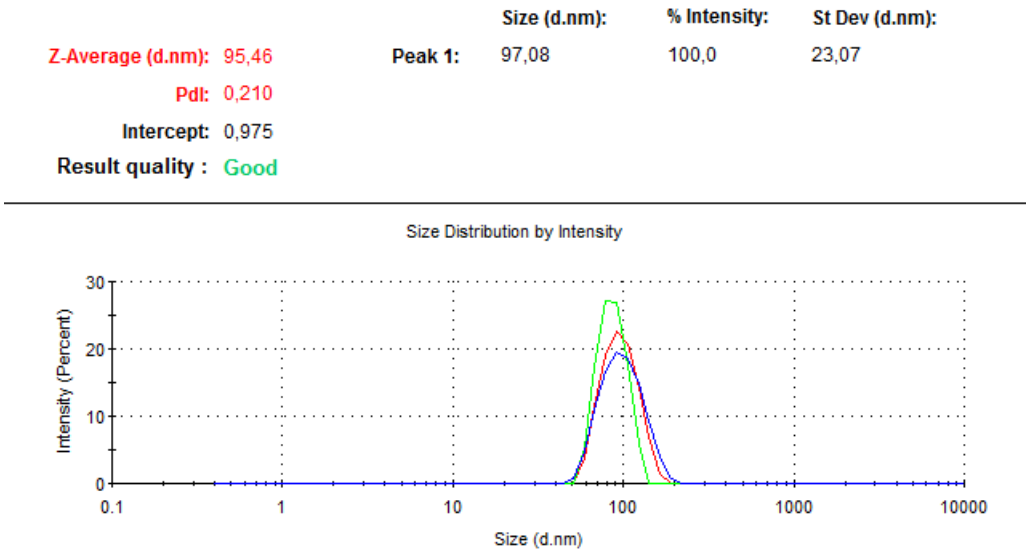

Figure 4.5: Example of a performed DLS measurement. The size distribution is based on the amount of scattered light in the sample. The result quality is also given after each measurement, as well as an average size of the particles. The coloured lines corresponds to three size measurements in a row.

In the example presented in Figure 4.5, the intensity being 100% tells that there are no liposomes with other sizes than 97.08nm ± 23.07nm present in the solution. However, what is missing from the DLS result and should be included in future measurements, is the zeta potential. This describes the charge of the produced liposomes which, in this case, would be of advantage since cationic liposomes are utilised. Due to technical problems with the zetasizer instrument, zeta potential was left out.

Three different types of lipids in four different compositions were tested at pH 5 and at physiological pH, see Table 4.1. Capture at physiological pH was only achieved for one specific composition, while immobilisation at pH 5 was successful for all tested compositions. One reason for this may be that the liposomes did not contain enough positive charges to electrostatically attract to the brushes at physiological pH. However, at pH 5, capture probably occurs by hydrogen bonding. The idea of hydrogen bonding seems not to work at physiological pH due to the brushes being deprotonated.

Table 4.1: Capture at pH 5 and physiological pH for different liposome compositions. None of the compositions could be fully released by applying electrical potentials. Lipid composition 1 and 3 are the only ones where the liposomes were completely released by switching to a solution with pH 11. Lipid composition 4 had only a small release at pH 11. Liposome sizes varied between 85-100nm.

Lipid composition (mol-%)	Capture pH 5	Capture pH 7.4	Release
1. 43% DPPC - 57% DOTAP	✓	0	pH 11
2. 20% DPPC - 80% DOTAP	✓	✓	-0.9V
3. 99% DPPC - 1% MVL5	✓	0	pH 11
4. 98% DPPC - 2% MVL5	✓	0	Incomplete

Results from QCM-D and SPR measurements for all compositions can be seen in Appendix A.4. However, lipid composition 2 and 3 shows some interesting behaviours. Injection of lipid composition 3 at pH 5 can be seen in Figure 4.6. A decrease in frequency is observed when the liposomes are injected, which means that mass is added to the brushes. Besides this, an increase in energy dissipation occurs. This tells that the brushes becomes more viscoelastic when the liposomes interact with them. A possible explanation might be the fact that liposomes also contain water. As a result, more water is present in the layer of brushes and therefore, the dissipation increases. Anyways, the liposomes were removed by testing both electrochemistry and pH 11, see Figure 4.6.

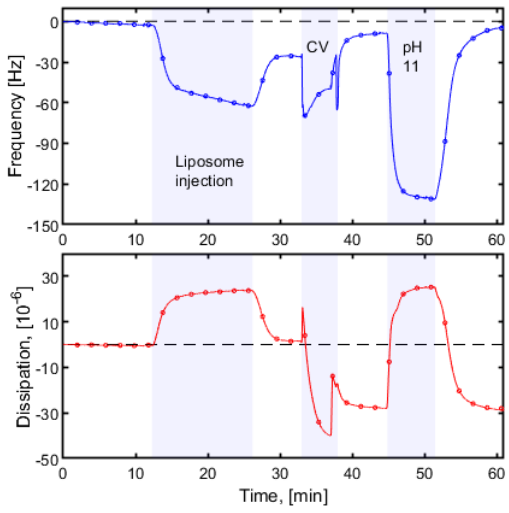

Figure 4.6: Immobilisation of lipid composition 3, at pH 5. Some of the liposomes were rinsed of with pH 5, while the rest were removed by both electrical potentials and pH 11.

By applying cyclic voltametry (CV) between 0V and -0.5V, a minimal amount of liposomes got released. In a CV-scan, the potential is sweeping between 0V and -0.5V

for the set time duration. A graph of this is presented in Figure A.4.4 in Appendix A.4. According to the frequency graph, the remaining liposomes were removed by injecting pH 11. At this pH, the brushes are deprotonated and can therefore not interact through hydrogen bonding anymore. Tests where pH was decreased to 2 were also performed, but no release could be observed.

Lipid composition 2 was in particular interesting, since that composition was the only one that resulted in successful interaction with the brushes at both pH 5 and physiological pH. At pH 5, liposomes were captured on the brushes and can be observed both in the frequency and dissipation. As previous figures have shown, the dissipation increase when liposomes are injected due to the brush layer becoming more viscoelastic. When the injection stopped, some liposomes were removed when the brush layer was rinsed with pH 5 solution, proving that some of them did not bind strong enough. To release the remaining, -0.5V was applied. According to the measurement, the electrical signal managed to release all of the liposomes. The result is presented in Figure 4.7.

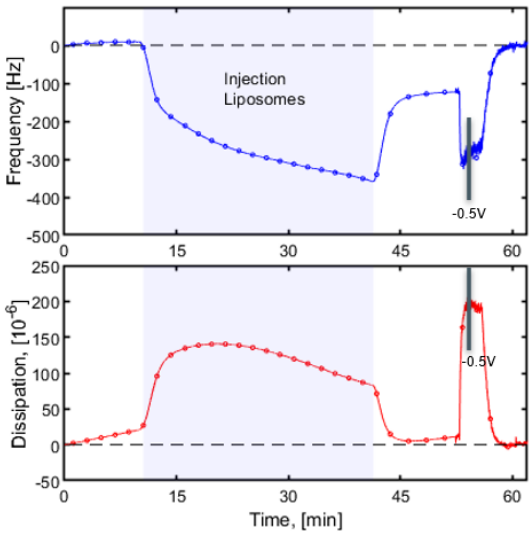

Figure 4.7: Successful capture and release at pH 5 of lipid composition 2. -0.5V was enough for the liposomes to release.

The liposomes with this composition were the only ones to be released with electrical signals at pH 5. Of all the tested compositions, lipid composition 2 contained the highest amount of cationic lipid. This may weaken the interaction with the brushes at pH 5 and the release will be easier.

The large quantity of cationic lipid in lipid composition 2 created the necessary electrostatic attraction for capture at physiological pH to occur. Based on the SPR measurement, capture was successful, see Figure 4.8.

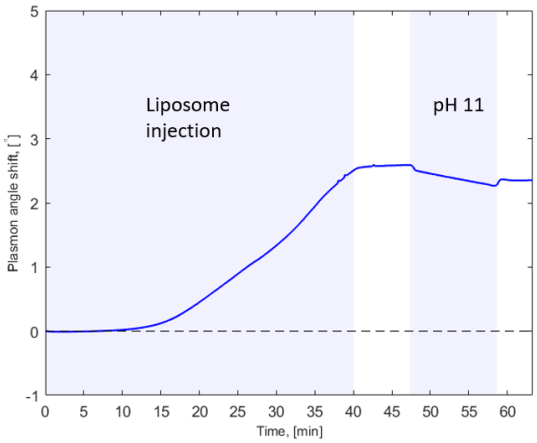

Figure 4.8: SPR measurement of lipid composition 2 at physiological pH. Injection of the liposomes lasted for 40 minutes and an unsuccessful release with pH 11 for 10 minutes.

In contrast to pH 5, the large amount of charges made release more difficult at physiological pH. This is probably due to the electrostatic attraction being stronger at physiological pH than the hydrogen bonds at pH 5. To study how the brushes behaved during the immobilisation and release of the liposomes, QCM-D measurement at physiological pH was performed and can be observed in the figure below.

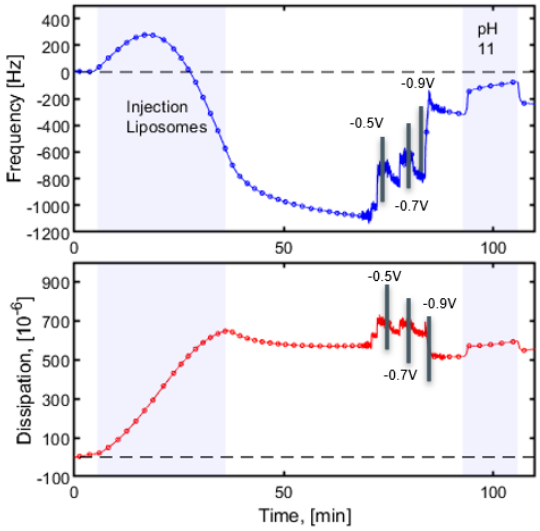

Figure 4.9: QCM-D measurement of lipid composition 2 liposomes. Frequency is increased when the potentials are applied while dissipation remains unchanged.

The measurement verifies the capture that was observed in the SPR, both in the frequency and dissipation. However, they differ when the liposomes are supposed to be released. According to the frequency, the applied electrical potentials and pH 11 manage to release a large amount since the graph is almost returning to the baseline. Still, the dissipation remain at the same level as before the electrical potentials were applied. It appears as the liposomes are released, but the brush layer remains

viscoelastic. This phenomenon is not well understood, and additional experiments have to be done to confirm this release behaviour. Although the release can be questioned, the capture of lipid composition 2 is observed in both the SPR and QCM-D measurements.

Lastly, it would also be of interest to know how many charges the liposomes carries. That knowledge would clarify the number of charges required to bind to the brushes at physiological pH. Thereby, one could optimise the liposome composition to achieve both capture and release. When release by switching to a pH 11 solution is accomplished, additional experiments involving electrochemistry can be executed. Also, one interesting experiment would be to test the same compositions, but instead creating liposomes of other sizes. This could give an indication whether the liposome size is an important parameter for interaction with the brushes, both regarding strength and space. Smaller liposomes have greater possibilities to interact with the brushes regarding to space, while larger binds stronger due to more charged groups.

5
Conclusion

In this project, two different strategies were tested to capture and release biomolecules at physiological pH. Initially, two types of poly(L)lysine with different molecular weights were tested. The first type had a larger molecular weight and resulted in non-favourable brush collapse that lead to difficulties to release the biomolecules. The second type was of lower molecular weight and could be captured and released from the brushes. Further, the carrier had a non-covalently attached biotin molecule. This allowed the carrier to interact with other biomolecules, such as neutravidin. The formed complexes were successfully captured on the brushes. Applied electrical potentials could release a significant amount, but pH 2 had to be injected for complete release.

The second strategy involved capture and release of self-manufactured liposomes. Several different lipid compositions were tested. Capture at pH 5 was successful for all compositions, but immobilisation at physiological pH was only successful for one of them. It contained 80% of the cationic lipid DOTAP and 20% of the zwitterionic lipid DPPC, making it the composition with largest quantity of DOTAP. Although capture was achieved, release was more difficult to confirm. One possible explanation might be that the liposomes contained many positive charges, resulting in a strong electrostatic attraction to the brushes. A possible way to trigger release of these kind of liposomes may be by lowering the positive net charge. Another composition, containing 53% DOTAP, resulted in unsuccessful capture at physiological pH. Therefore, producing liposomes with a DOTAP composition between 53%-80% would be of interest.

To conclude, the two strategies are of high relevance for capture and release of biomolecules. PLL with lower molecular weight has been proven to bind to the brushes at physiological pH. Another advantage with PLL is the possibility to use reactive end groups, making it adjustable for specific purposes. Although, due to the difficulties to completely release with electrochemistry, more research involving longer time periods of applied potentials and even lower molecular weight PLL have to be studied. Compared to PLL, liposomes require further understanding. Performed measurements have proven that liposomes can interact with the brushes at physiological pH, but releasing them was challenging. Therefore, additional testing about the importance of liposome size and charge have to be done. By knowing the size and the charge for different compositions, modifications can be done to produce optimal liposomes for the task as biomolecule carrier.

Bibliography

1. Dohnhammar, U., Reeve, J. & Walley, T. *Patients' expectations of medicines - a review and qualitative synthesis* Apr. 2016.
2. Raj Shukla. *New Automated Purification Strategies for Scale-Up* Dec. 2017.
3. Walker, N. 2016 Pharmaceutical Equipment Buying Trends. *Pharmamanufacturing* (July 2016).
4. Glass, T. *Avoiding Contamination and Particulate Build Up in Pharmaceutical Manufacturing* Aug. 2017.
5. Urh, M., Simpson, D. & Zhao, K. in *Methods in Enzymology* 417–438 (2009).
6. Burdick, R. *What Are the Disadvantages of HPLC?* 2018.
7. Wand, A. *Cost-Effective Chromatography* 2018.
8. Kinsella M. Joseph, I. A. Taking charge of biomolecules. *Nature Nanotechnology* **2,** 596–597 (2007).
9. Voon, C. H. & Sam, S. T. in *Nanobiosensors for Biomolecular Targeting* 23–50 (Elsevier, 2019).
10. Scalschi, L. *et al.* 1-Methyltryptophan Modifies Apoplast Content in Tomato Plants Improving Resistance Against Pseudomonas syringae. *Frontiers in Microbiology* **9.** ISSN: 1664-302X (Aug. 2018).
11. Castillo, G. F.-d. *Polyelectrolyte Brush Electrodes for Protein Capture and Release* tech. rep. (2020).
12. Milner, S. T. Polymer Brushes. *New Series* **22,** 905–914 (1991).
13. Jones L. A. Richard. *Soft Condensed Matter* 1st, 77–87 (Oxford University Press, 2002).
14. Minko, S. *Grafting on Solid Surfaces: "Grafting to" and "Grafting from" Methods* 1st (ed Stamm, M.) 215–234 (Springer, Dresden, 2008).
15. Ballauff, M. & Borisov, O. Polyelectrolyte brushes. *Current Opinion in Colloid and Interface Science* **11,** 316–323. ISSN: 13590294 (Dec. 2006).
16. Das, S., Banik, M., Chen, G., Sinha, S. & Mukherjee, R. Polyelectrolyte brushes: theory, modelling, synthesis and applications. *Soft Matter* **11,** 8550–8583. ISSN: 1744-683X (2015).
17. Nová, L., Uhlík, F. & Košovan, P. Local pH and effective pKA of weak polyelectrolytes-insights from computer simulations. *Physical Chemistry Chemical Physics* **19,** 14376–14387. ISSN: 14639076 (2017).
18. Wu, T. *et al.* Behavior of surface-anchored poly(acrylic acid) brushes with grafting density gradients on solid substrates: 1. Experiment. *Macromolecules* **40,** 8756–8764. ISSN: 00249297 (Nov. 2007).
19. Ferrand-Drake del Castillo, G., Hailes, R. L. N. & Dahlin, A. Large Changes in Protonation of Weak Polyelectrolyte Brushes with Salt Concentration—Implications

for Protein Immobilization. *The Journal of Physical Chemistry Letters* **11,** 5212–5218. ISSN: 1948-7185 (July 2020).

20. Ferrand-Drake Del Castillo, G., Emilsson, G. & Dahlin, A. Quantitative Analysis of Thickness and pH Actuation of Weak Polyelectrolyte Brushes. *Journal of Physical Chemistry C* **122,** 27516–27527. ISSN: 19327455 (2018).
21. Ferrand-Drake del Castillo, G., Adali, Z., L. N. Hailes, R., Xiong, K. & Dahlin, A. Generic High-Capacity Electrochemical Capture and Release of Proteins by Polyelectrolyte Brushes. *ChemRxiv* (2020).
22. Novák, P. & Havlíček, V. in *Proteomic Profiling and Analytical Chemistry* 51–62 (Elsevier, 2016).
23. Volodkin, D., Ball, V., Schaaf, P., Voegel, J. C. & Mohwald, H. Complexation of phosphocholine liposomes with polylysine. Stabilization by surface coverage versus aggregation. *Biochimica et Biophysica Acta - Biomembranes* **1768,** 280–290. ISSN: 00052736 (Feb. 2007).
24. Batys, P., Morga, M., Bonarek, P. & Sammalkorpi, M. PH-Induced Changes in Polypeptide Conformation: Force-Field Comparison with Experimental Validation. *Journal of Physical Chemistry B* **124,** 2961–2972. ISSN: 15205207 (Apr. 2020).
25. Hermanson, G. T. *Introduction to Bioconjugation* 1–125. ISBN: 9780123822390 (2013).
26. Akshay J & Cheng K. The principles and applications of avidin-based nanoparticles in drug delivery and diagnosis. *Physiology & behavior* **176,** 139–148 (2017).
27. Scioli Montoto, S., Muraca, G. & Ruiz, M. E. Solid Lipid Nanoparticles for Drug Delivery: Pharmacological and Biopharmaceutical Aspects. *Frontiers in Molecular Biosciences* **7.** ISSN: 2296889X (Oct. 2020).
28. Akbarzadeh, A. *et al.* Liposome: Classification, preparation, and applications. *Nanoscale Research Letters* **8.** ISSN: 1556276X (2013).
29. Rajappan, K. *et al.* Property-Driven Design and Development of Lipids for Efficient Delivery of siRNA. *Journal of Medicinal Chemistry* **63,** 12992–13012. ISSN: 0022-2623 (Nov. 2020).
30. Su, R. *et al. Reference Module in Biomedical Sciences* (Elsevier, 2021).
31. Perry, S. C. *et al.* Electrochemical synthesis of hydrogen peroxide from water and oxygen. *Nature Reviews Chemistry* **3,** 442–458. ISSN: 23973358 (July 2019).
32. Bakhtiar, R. Surface plasmon resonance spectroscopy: A versatile technique in a biochemist's toolbox. *Journal of Chemical Education* **90,** 203–209. ISSN: 00219584 (Feb. 2013).
33. A. B. Dahlin. *Advances in Biomedical Spectroscopy* 77–89 (IOS Press, 2012).
34. Weik, M. H. *Computer science and communications dictionary* 2006. ISBN: 1402006136 (Kluwer Academic Publishers, 2000).
35. Peterson, A. W., Halter, M., Plant, A. L. & Elliott, J. T. Surface plasmon resonance microscopy: Achieving a quantitative optical response. *Review of Scientific Instruments* **87.** ISSN: 10897623 (Sept. 2016).
36. Tonda-Turo, C., Carmagnola, I. & Ciardelli, G. Quartz crystal microbalance with dissipation monitoring: A powerful method to predict the in vivo behavior

of bioengineered surfaces. *Frontiers in Bioengineering and Biotechnology* **6,** 1–7. ISSN: 22964185 (2018).

37. Höök, F. & Kasemo, B. in *Piezoelectric Sensors* July 2006, 425–447 (Springer Berlin Heidelberg, 2007). ISBN: 978-3-540-36568-6.
38. Dixon, M. C. Brief background And History of QcM Quartz Crystal Microbalance with Dissipation Monitoring: Enabling Real-Time Characterization of Biological Materials and Their Interactions. *Journal of Biomolecular Techniques* **19,** 151–158 (2008).
39. Nanoscience Instruments. *Electrochemical Quartz Crystal Microbalance with Dissipation Monitoring (EQCM-D)*
40. *Two-, Three-, and Four-Electrode Experiments* Apr. 2011.
41. Maeda, S., Fujiwara, Y., Sasaki, C. & Kunimoto, K. K. Structural analysis of microbial poly(ϵ-L-lysine)/poly(acrylic acid) complex by FT-IR, DSC, and solid-state 13C and 15N NMR. *Polymer Journal* **44,** 200–203. ISSN: 00323896 (Feb. 2012).
42. Parker, F. S. in *Applications of Infrared Spectroscopy in Biochemistry, Biology, and Medicine* 165–172 (Springer US, Boston, MA, 1971).

A

Appendix 1

A.1 Chemicals

Chemicals used for all experiments were:

- Milli-Q® water (18.2MΩ cm, Millipore)
- EtOH (95%)

Following chemicals were used in the synthesis of diazonium salt and of PAA brushes:

- $\alpha-$bromoisobutylbromide (98%, Sigma-Aldrich)
- Acetonitrile (99.8% Sigma-Aldrich)
- Aminophenetyl alcohol (98% Sigma-Aldrich)
- Ammonium hydroxide (Acros Organics)
- Chloroform (+99.5% Alfa Aesar)
- Copper(II)bromide (99% Sigma-Aldrich)
- DCM (+99% Acros Organics)
- Diethyl ether (≥99.7% Sigma-Aldrich)
- DMSO (≥99.5% Sigma-Aldrich)
- DOTAP (>99% M_w = 698.542 Avanti Polar Lipids®)
- DPPC (>99%, M_w = 734.039 Avanti Polar Lipids®)
- Hydrogen peroxide (35% Scharlab)
- Hydroquinone (99%)
- L-ascorbic acid (≥99% Sigma-Aldrich)
- Methanesulfonic acid (≥99% Sigma-Aldrich)
- MVL5 (>99%, M_w = 1164.862 Avanti Polar Lipids®))
- Neutravidin
- PMDETA (99% Sigma-Aldrich)
- Poly(L)lysine hydrogenbromide ($M_w \sim$ 30 000-70 000g/mol Sigma-Aldrich)
- Poly(L)lysine hydrochloride biotin (M_w = 3300g/mol Nanosoft polymers)
- PBS (Sigma-Aldrich)
- Sulfuric acid (95%-98% Sigma-Aldrich)
- TBA (98% Sigma-Aldrich)
- TBN
- Tetrafluoroboric acid (40% in H_2O Honeywell)
- Toluene (99.8% Sigma-Aldrich)
- Triethylamine (≥99.7% Sigma-Aldrich)

A.2 Fresnel modelling

Transformation matrix Φ with the indicator m, that corresponds to the number of materials, while j shows at what interface the Fresnel coefficient is calculated.

$$\Phi = \prod_{j=2}^{m-1} \left(\frac{1}{F_{t,[m-1]m}} \begin{bmatrix} 1 & F_{r,[j-1]j} \\ F_{r,[j-1]j} & 1 \end{bmatrix} \times \begin{bmatrix} e^{-ik_0 d_j cos(\theta_j)} & 1 \\ 1 & e^{-ik_0 d_j cos(\theta_j)} \end{bmatrix} \times \frac{1}{F_{t,[m-1]m}} \begin{bmatrix} 1 & F_{r,[m-1]m} \\ F_{r,[m-1]m} & 1 \end{bmatrix} \right) \tag{A.1}$$

The reflection or transmission for a specific layer is calculated according to the equations below.

$$F_r = \frac{\Phi(2,1)}{\Phi(1,1)} \tag{A.2}$$

$$F_t = \frac{1}{\Phi(1,1)} \tag{A.3}$$

An example of a Fresnel modelling calculation is given in Figure A.1 below. The brush height, or thickness, is based on a model that uses experimental data.

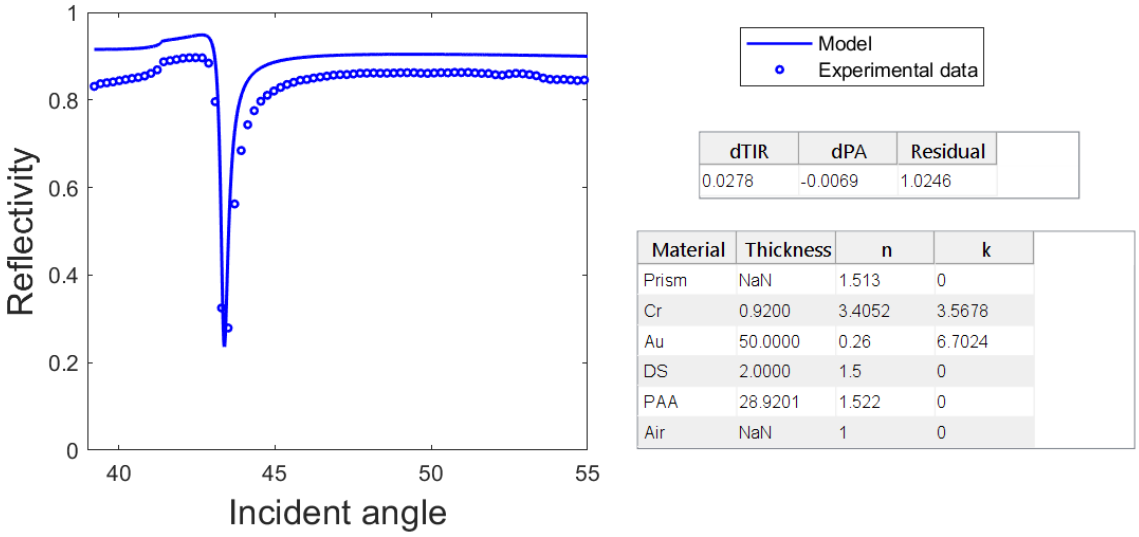

dTIR	dPA	Residual
0.0278	-0.0069	1.0246

Material	Thickness	n	k
Prism	NaN	1.513	0
Cr	0.9200	3.4052	3.5678
Au	50.0000	0.26	6.7024
DS	2.0000	1.5	0
PAA	28.9201	1.522	0
Air	NaN	1	0

Figure A.1: Height estimation based on Fresnel modelling. n corresponds to refractive index while k is a constant. The different materials in the SPR sensor are chromium, gold, diazonium salt and PAA brushes. All of the values, except PAA thickness, are literature values.

A.3 BSA injection

To ensure that electrochemistry was applicable, a test involving capture and release of the biomolecule BSA, was performed. This confirmed that a great amount of biomolecules could be immobilised and later released by applying +0.5V and +0.6V for 180s.

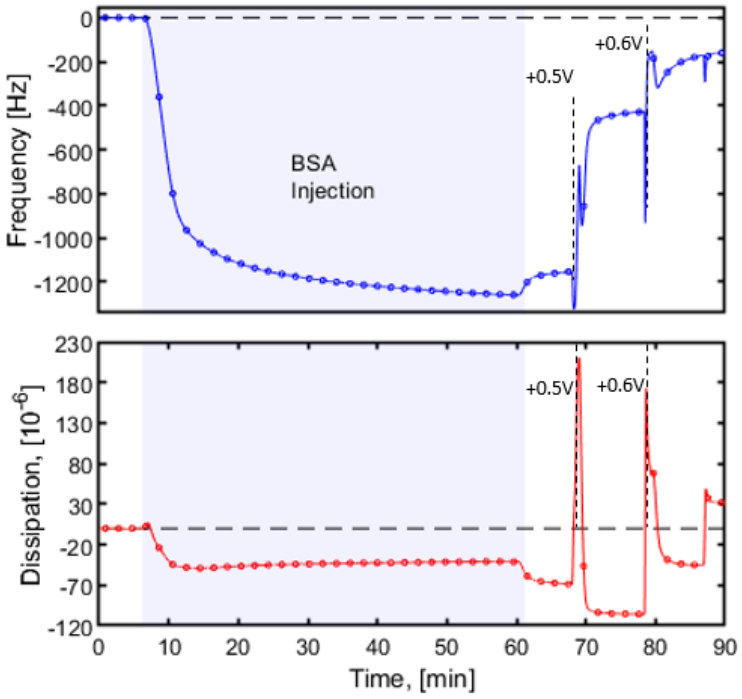

Figure A.2: Capture and release of BSA.

A.4 Liposome injections

All of the injections of the samples are presented in the upcoming figures. Sample 1 was succesfully captured and released at pH 5, see Figure A.4.1.

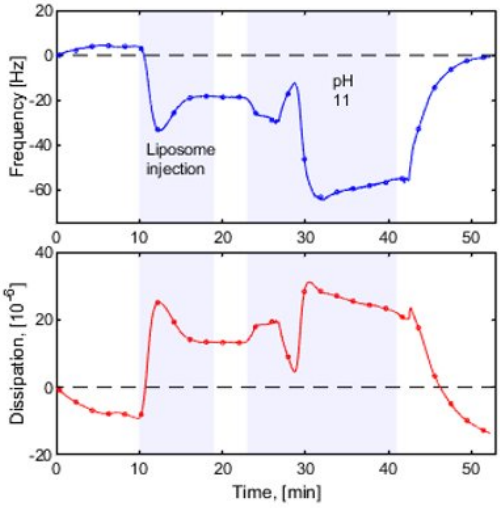

Figure A.4.1: Injection of 43% DPPC and 57% DOTAP liposomes at pH 5.

Sample 4 had a small increase in SPR angle, indicating that some liposomes were interacting with the brushes. Only few were released with pH 11, see Figure A.4.2.

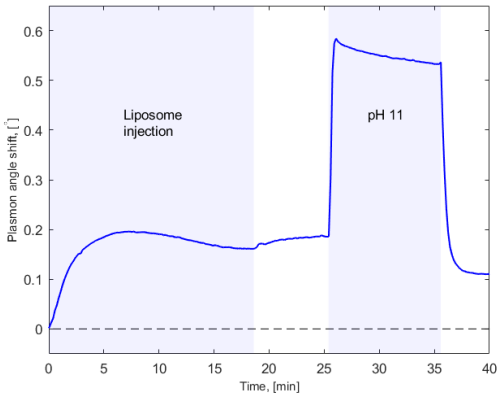

Figure A.4.2: Liposomes consisting of 98% DPPC and 2% MVL5 are immobilised on the brushes at pH 5. Unsuccessful release at pH 11.

There were several measurements performed at physiological pH, where only sample 2 resulted in capture. One example of how the measurements looked like, when no liposomes were interacting, can be seen in Figure A.4.3.

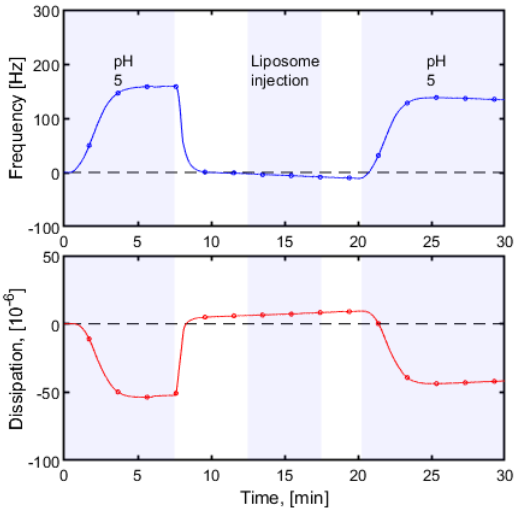

Figure A.4.3: Injection of 99% DPPC and 1% MVL liposomes at physiological pH.

For one of the samples, a CV-scan measurement was performed. In the example measurement below, the voltage swept between 0V and -0.5V three times. The voltage generates a current, given on the y-axis.

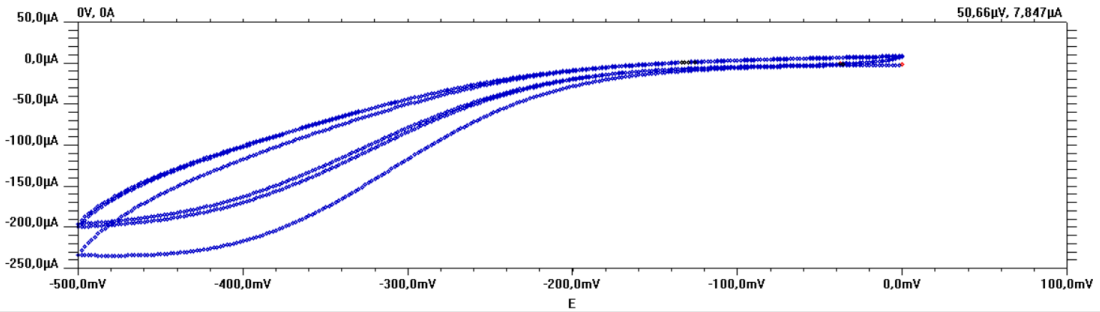

Figure A.4.4: CV-scan measurement

A.5 IR verification of PLL on PAA

To verify that PLL was electrostatically interacting with the brushes, IR measurements were performed.

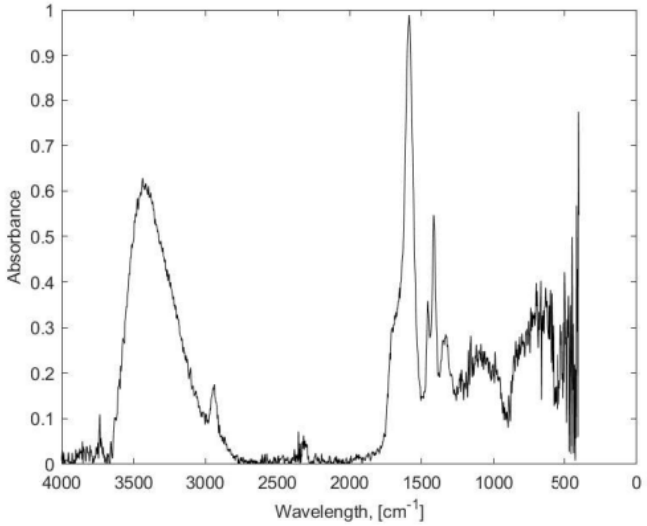

Figure A.5.1: IR spectrum of PAA brushes. The high peaks around 1700cm^{-1} corresponds to the carbonyl group on PAA.[41]

By comparing Figure A.5.1 and Figure A.5.2a, the characteristic peaks of PLL is showed. The peaks are highlighted in Figure A.5.2b. 1657cm^{-1} and 1564cm^{-1} corresponds to the amide peaks.[41][42]

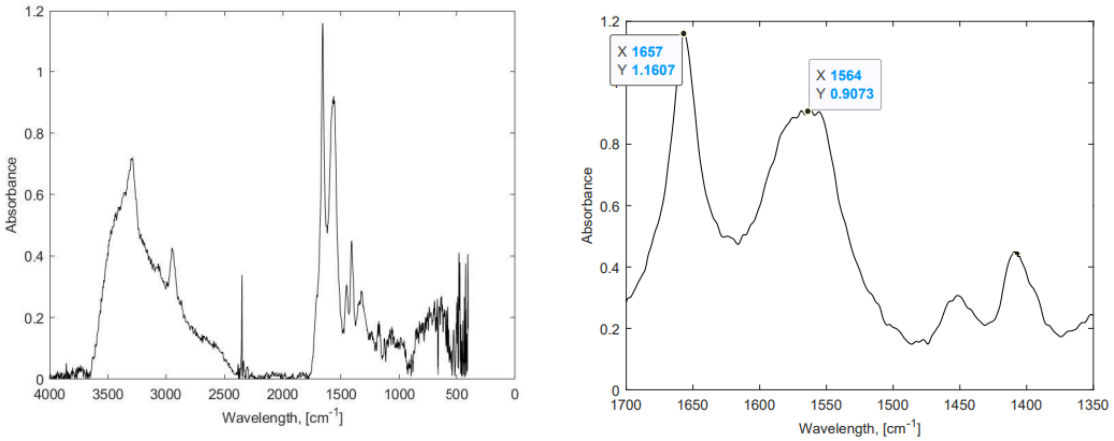

(a) IR spectrum of PLL on the brushes.

(b) Highlight of the amide and carboxylate peaks.

Figure A.5.2: IR spectrum of PLL on PAA brushes. Characteristic peaks of PLL are seen in Figure A.5.2b.

DEPARTMENT OF APPLIED CHEMISTRY
CHALMERS UNIVERSITY OF TECHNOLOGY
Gothenburg, Sweden
www.chalmers.se

CHALMERS
UNIVERSITY OF TECHNOLOGY